ACOUSTIC RESONANCE IN AN INDEPENDENT-GATE FINFET

Dana Weinstein[1*] *and Sunil A. Bhave*[2]
[1]Massachusetts Institute of Technology, Cambridge, Massachusetts, USA
[2]Cornell University, Ithaca, New York, USA

ABSTRACT

This paper demonstrates the acoustic resonance of an Independent-Gate (IG) FinFET driven with internal dielectric transduction and sensed by piezoresistive modulation of the drain current through the transistor. An acoustic resonance at 37.1 GHz is obtained with a quality factor of 560, corresponding to an *f.Q* product of 2.1×10^{13}. The demonstrated hybrid NEMS-CMOS technology can provide RF CMOS circuit designers with high-*Q* active devices operating up to mm-wave frequencies and beyond.

INTRODUCTION

As we scale to deep sub-micron (DSM) technology, transistor unity gain frequencies increase, enabling the design of CMOS circuits for RF and mm-wave applications up to 95 GHz. However, such high-frequency CMOS transistors have limited gain, resulting in poor output power efficiency. Successful implementation of DSM CMOS in mm-wave applications therefore requires high-*Q*, low-power components operating at high frequencies.

Another challenge facing DSM circuits is the increasing density of devices, projected to reach 10^{11} devices/cm^2. At such densities, clock distribution and the power consumption associated with it necessitate implementation of low-power local clocks with the potential for global synchronization. The Resonant Body Transistor (RBT) presented in this work is a fundamental building block that addresses both these challenges.

Field effect transistors (FETs) were first used for sensing mechanical motion in one of the earliest Micro Electromechanical (MEM) devices. In 1967, Nathanson et al. demonstrated the Resonant Gate Transistor (RGT), driving resonance in a gold cantilever with an air-gap capacitive electrode [1]. The RGT cantilever functioned as the gate of an air-gap transistor, with output drain current modulated by the cantilever resonant motion. This device achieved a resonance frequency of 30 kHz with quality factor of ~70 despite the limited processing capabilities of the time. Fabrication limitations prevented the proliferation of these and other MEMS devices until the advent of silicon-based surface micromachining.

FET sensing has only recently regained momentum as a means of mechanical detection, and has been implemented in a variety of micromechanical devices. Resonant Gate Transistors similar to Nathanson's device have been demonstrated in silicon air-gap resonators up to 14 MHz [2,3]. Mechanical resonators sensed through direct elastic modulation of a transistor channel have also been demonstrated. Such devices include air gap resonators with FETs embedded in the resonator body up to 71 MHz [4], mechanical mixing in single electron transistors up to 245 MHz [5], and piezoelectric high electron mobility transistor (HEMT) channel modulation in GaN resonators up to 2 MHz [6].

Internal Dielectric Transduction

To improve electrostatic transduction efficiency and scale MEM resonators into the GHz domain, we previously demonstrated longitudinal silicon bar resonators using a novel method to drive and sense acoustic waves in the bar. This mechanism, termed 'internal dielectric transduction' [7], incorporates thin dielectric film transducers inside the resonator body for capacitive transduction. Internal dielectrically transduced resonators have yielded acoustic resonance frequencies up to 6.2 GHz [8] and frequency-quality factor products (*f.Q*) up to 5.1×10^{13} [9]. Moreover, these dielectrically transduced resonators demonstrate improved efficiency as resonance frequency increases, providing a means of scaling MEM resonators to previously unattainable frequencies. However, at multi-GHz frequencies capacitive feed-through becomes significant and prevents capacitive detection of MEM resonance without three-port mixing measurements.

Unlike capacitive sensing employed in these resonators, FET sensing can amplify the mechanical signal prior to any feed-through parasitics. Combining the benefits of FET sensing with the frequency scaling and high-*Q* capabilities of internal dielectrically transduced resonators, the authors recently demonstrated a Resonant Body Transistor (RBT) [10] operating at 11.7 GHz with *Q* of over 1800. This device incorporates a field-effect transistor into the resonator body for internal amplification of the resonant signal. The best RBT geometry for optimal dielectric transduction at high frequencies is an internal dielectrically transduced longitudinal-mode resonator, with dielectric films positioned at points of maximum strain. As we scale to higher frequency, the width of the resonator decreases, eventually converging to a geometry very similar to that of Independent-Gate FinFETs [11].

THE RESONANT BODY TRANSISTOR

Theory

The principle of operation of the internal dielectrically transduced RBT is shown in Fig. 1. The region in light grey represents the active region of the resonator, while the blue region is highly doped. The active region near the drive gate is biased into accumulation (red), so that a large capacitive force acts across the thin dielectric film (yellow), driving longitudinal vibrations in the body. A gate voltage is applied to the opposing gate, generating an inversion channel (blue) which results in a DC drain current. At resonance, elastic waves formed in the resonator modulate the drain current both by physically changing the gate capacitance and by piezoresistive modulation of carrier mobility. The internally amplified RBT has significantly lower output impedance than capacitive detection mechanisms, simplifying impedance matching with active circuits.

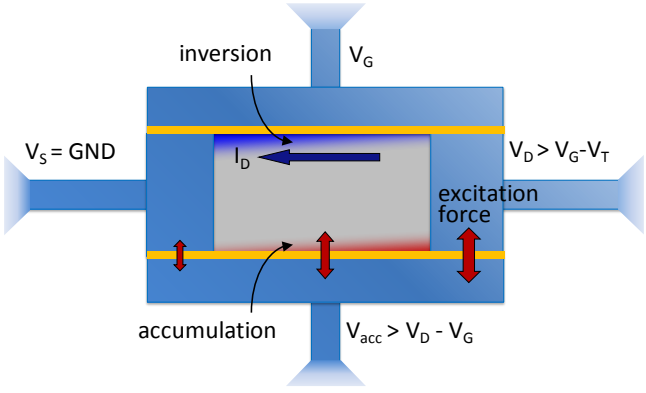

Fig. 1. *Top-view schematic showing principle of operation of a bulk-mode dielectrically transduced Resonant Body Transistor. The RBT geometry, similar to that of an IG-FinFET, incorporates FET sensing with a dielectrically transduced bar resonator.*

The amplitude of vibrations of the internal dielectrically transduced RBT $U_0|_{RBT}$ can be found in an analysis similar to [7] and has been investigated in [10]. The strain induced in the resonator piezoresistively modulates the drain current running through the inversion layer. Assuming a piezoresistive coefficient of π_{110} for current traveling perpendicular to the normal of elastic wave fronts along <110>, the change in mobility is given by

$$\frac{d\mu_n}{\mu_n} = \pi_{110} Y \frac{\partial u}{\partial x}\Big|_{invers\ ion} = \pi_{110} Y k_n U_0|_{RBT} \cos\left(\frac{1}{2} k_n g\right). \quad (1)$$

where g is the dielectric thickness, Y is the Young's modulus and k_n is the wave number of the n[th] harmonic. The piezoresistive mobility modulation of Eqn. 1 generates an AC current linearly dependent on the drain current:

$$i_{out}|_{RBT} \approx I_D \frac{\partial \mu_n}{\mu_n} \quad (2)$$

The electromechanical transconductance is defined by

$$g_{m,em} \equiv i_{out}|_{RBT} / v_{in} \ . \quad (3)$$

One of the fundamental obstacles of scaling MEMS resonators to multi-GHz frequencies is the need for a sense transducer that overcomes feed-through and parasitic capacitance and provides adequate sensitivity to measure mechanical motion at those frequencies. Fig. 2(a) shows a standard Butterworth-Van Dyke (BVD) model of a capacitively transduced resonator whose output is fed into a common source amplifier. As electrostatically transduced resonators shrink in size to scale to GHz frequencies, the feed-through capacitance C_{FT} limits the minimum detectable electromechanical signal through the device. In Fig. 2(a), both the feed-through current and electromechanical current are amplified in the amplifier following the resonator, making 2-port detection impossible at high frequencies.

The linear equivalent circuit (LEC) of a dielectrically driven RBT is given in Fig. 2(b). This model differs from that of a standard MOSFET in two ways. First, the AC electrical signal is applied to the back gate (B) biased in accumulation, leaving the inversion gate (G) at a constant bias voltage. This biasing prevents the input signal from electrically modulating the inversion channel. Second, the small signal current source is not a constant function of frequency. In this model, the electromechanical transconductance $g_{m,em}$ has a Lorentzian frequency dependence with peak amplitude defined by Eqn. 3 and a mechanical quality factor $Q_m = 1/R_X \sqrt{L_X/C_X}$ as in the case of the standard BVD model. The capacitive feed-through in the RBT is just the parasitic

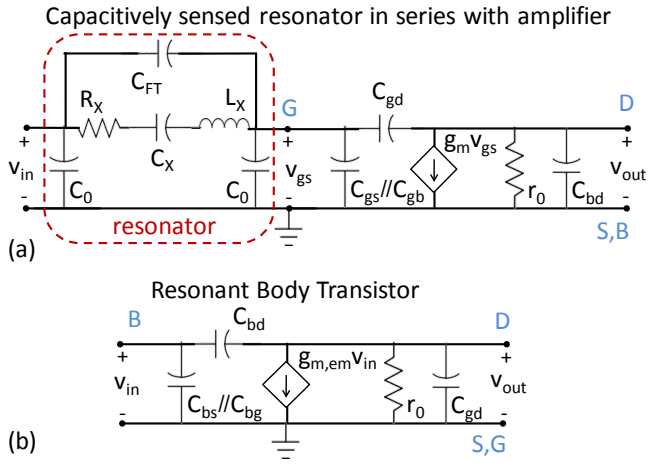

Fig 2. *Small signal model of (a) a capacitively sensed resonator with an external single-stage amplifier, and (b) a Resonant Body Transistor, with resonance incorporated into $g_{m,em}$.*

C_{bg}, C_{bs}, and C_{bd}. Due to the symmetry of the RBT, C_{bs} and C_{bd} are equivalent to C_{gs} and C_{gd} found in the amplifier of Fig. 2(a). Moreover, the feed-through component C_{bg} in the fully depleted RBT, equal in magnitude to C_{FT}, is not amplified in any way. Therefore, integration of FET sensing into the acoustic resonator enables amplification of the electromechanical signal without amplification of electrical feed-through.

Independent-Gate FinFET Resonance

Many three-dimensional transistors such as nanowire FET and tri-gate and independent gate FinFETs are currently under development for future CMOS nodes. As the RBT realized in [10] scales to higher frequencies, the length direction (perpendicular to the drain current in device) decreases resulting in a structure very similar to an Independent-Gate (IG) FinFET. However, resonant transistors are not limited to this topology; the drive and sense mechanisms in the RBT can be extended to acoustically resonate transistors of various geometries and materials.

In this paper, we demonstrate the acoustic resonance of the released IG-FinFET similar to that shown in Fig. 3, with a single-crystal silicon fin of 114 nm width and 220 nm thickness and two polysilicon gates. The gate dielectrics are composed of 15 nm silicon nitride on either side of the fin. As in the case of the RBT, one gate of the IG-FinFET is biased into accumulation to drive acoustic waves in the device. The other gate biases the fin into inversion to generate a drain current for FET sensing of the elastic waves. The active area of this n-type device is lightly p-doped ($N_A = 10^{14}$ cm^{-3}) while gates, source, and drain are highly doped with As ($N_D \sim 10^{18}$ cm^{-3}).

After the HF release of the device, both fin and gates are freely suspended and can resonate in contour plate modes defined by the composite geometry of the gates and fin. Each gate of the demonstrated device measured 500 nm (gate length along the fin) by 400 nm. While many plate modes may be possible in this structure, the longitudinal waves generated perpendicular to the dielectric film reduces the number of modes excited by dielectric transduction of the device. Moreover, the FET sensing averages the distributed piezoresistive contribution of strain to the total AC drain current along a small region of the device (along the FET channel) resulting in a further reduction of undesired modes detected at the output.

A harmonic analysis of the IG-FinFET was performed in COMSOL Multiphysics to determine the resonance modes which could be both excited and detected in the device. A harmonic force of 2.7x10^5 N/m^2 was applied along both interfaces of one dielectric film to simulate the electrostatic force on the accumulation side of the fin. This corresponds to an accumulation gate voltage $V_{ACC} = -1\ V$, a drain voltage $V_D = 4\ V$, a grounded source, and an AC

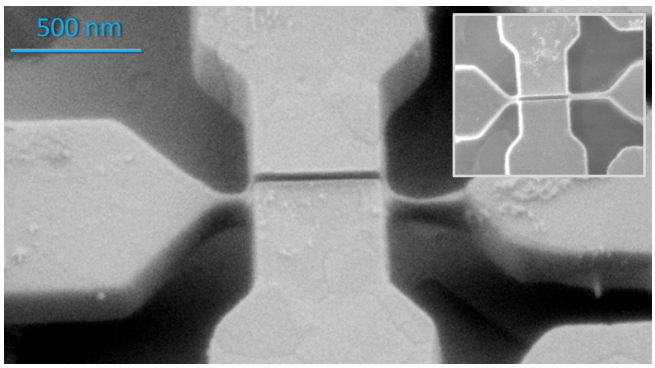

Fig. 3. *Scanning electron micrograph of a suspended independent-gate FinFET. The devices have a gate length of 500 nm.*

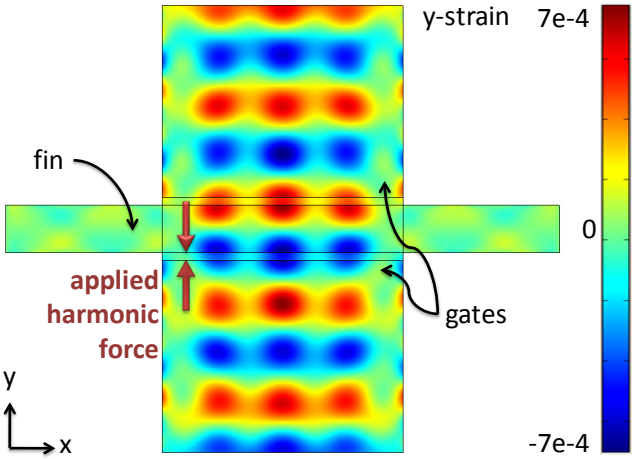

Fig. 4. *COMSOL harmonic analysis of released IG-FinFET structure. Simulation shows the y-axis strain due to harmonic force applied across the lower dielectric film at the resonance frequency. Due to symmetry of the mode, the x-axis strain does not contribute to the piezoresistive signal. This mode corresponds to the half-wavelength resonance of the fin width (width-extensional mode).*

excitation at the accumulation gate of $v_{in} = 0.4\,V$. There is a roughly linear voltage drop from drain to source along the fin, resulting in a electrostatic force gradient along the dielectric. In the harmonic analysis, this is approximated as an averaged voltage evenly distributed along the length of the capacitor. The direction of the harmonic forces applied is shown in Fig. 4.

A frequency sweep from 30 to 50 GHz resulted in about 8 resonance modes excited from the force on the dielectric film. To determine the subset of these modes that would be detected with piezoresistive FET sensing, the strain was integrated along the fin at the region of inversion. As illustrated in Fig. 1, the inversion region exists inside the fin at the interface to the second dielectric film not used for driving resonance. Integration along this interface reduced the number of detectable eigenmodes to three in the simulation range of 20 GHz. Fig. 4 shows a contour plot of the y-axis strain of a contour mode resonance with acoustic half-wavelength corresponding to the width of the fin.

This simulated contour mode of the IG-FinFET at 35 GHz in Fig. 4 shows a 10th harmonic longitudinal mode in the y-direction coupled to a 7rd harmonic in the x-direction. Fig. 5 provides displacement and strain plots extracted from this mode across the fin. An AC drain current through the fin can result from both transverse (y-direction) and longitudinal (x-direction) strain acting piezoresistively on the drain current flowing in the x-direction. The simulated mode exhibits both positive and negative strain in the x-direction, resulting in cancelation of piezoresistive contribution to the drain current from longitudinal strain. The transverse strain inside the fin generated by its λ/2 resonance is both tensile and compressive. However, the current flowing through the fin is confined to the inversion region near one of the dielectrics, where the transverse strain is largely uniform along the length of the fin. This contributes to a net piezoresistive change in drain current at the resonance frequency.

In accordance with the theory of internal dielectric transduction, the harmonic response of the structure results in maximum strain and corresponding displacement nodes at the dielectric transducers. This configuration of drive (capacitive) and sense (piezoresistive) transducers yields the highest efficiency conversion from the electrical to mechanical domain and back into an electrical signal.

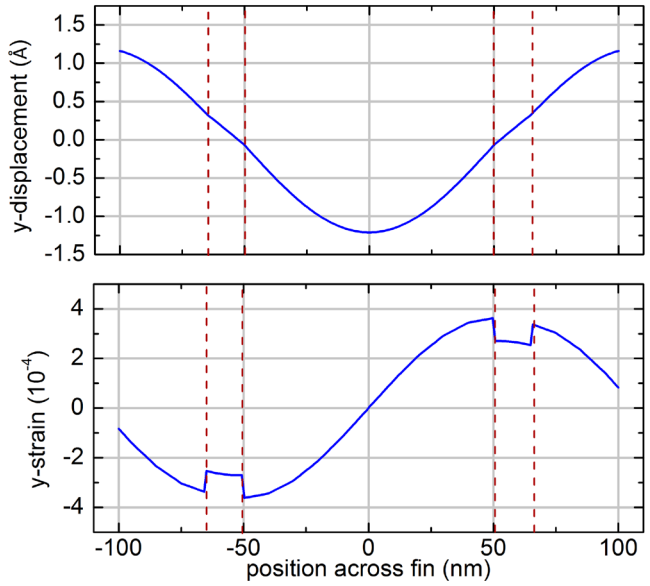

Fig. 5. *COMSOL simulation of displacement and strain in y-direction across the 100 nm fin (± 50 nm). Dashed lines indicate position of 15 nm dielectric films, extending into the gate silicon beyond ± 65 nm.*

MEASUREMENT

The devices were tested in a two-port configuration at room temperature in a vacuum probe station, as shown in Fig 6. The resonating IG-FinFET is represented by a new RBT symbol. This symbol of the 4-terminal device illustrates the contribution of mechanical resonance from the back gate to the characteristics of the transistor channel.

The devices were tested in vacuum to prevent ionization of air in the fringe fields near the dielectric, where up to 5 V were applied across a 15 nm gap. The vacuum also prevented adsorption of molecules onto the surface of the resonator over time, which can degrade the quality factor. After de-embedding the device from the probe pads and routing, the transconductance is obtained from the Y-parameters, $g_m = Y_{21} - Y_{12}$, as in the case of conventional transistor measurements. A detailed explanation of the de-embedding structures and algorithm is provided in the supplementary material of [10].

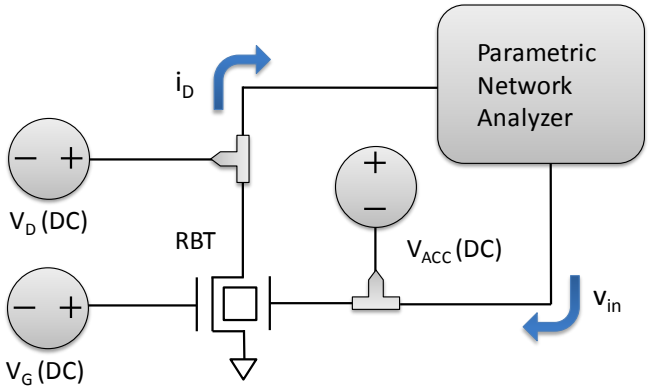

Fig. 6. *Schematic of 2-port measurement for frequency characterization of RBT. The drive and sense gates of the RBT were biased into accumulation and inversion, respectively. An AC excitation was superimposed on the drive gate using a parametric network analyzer.*

EXPERIMENTAL RESULTS

IG-FinFETs were fabricated side-by-side with bar RBTs demonstrated in [10] in an SOI process similar to that used in standard CMOS processing. While the bar-geometry RBTs have polysilicon gates patterned to define the resonance frequency, the poly gates of the IG-FinFETs extend uniformly to the metal contacts, as seen in Fig. 3. The resonance frequency of the IG-FinFET corresponds to the width-extensional mode of the transistor fin. All IG-FinFETs have a gate length of 500 nm and a device thickness of 220 nm. The active area of the FETs is lightly p-doped ($N_A = 10^{14}$ cm^{-3}), resulting in fully-depleted devices.

The measured frequency response of one IG-FinFET is shown in Fig. 7, applying an accumulation gate voltage $V_{ACC} = -1\,V$, a drain voltage $V_D = 4\,V$, and an AC excitation at the accumulation gate of -18 dBm or $v_{in} = 0.4\,V$. The measured response is given in terms of the back gate transconductance g_{mb}, highlighting the fact that the excitation is applied to the back gate. This is done in order to isolate the electrical input signal from the output. The resonance peak is attributed to the frequency-dependent electromechanical transconductance $g_{m,em}$ due to piezoresistive modulation of the drain current. The signal floor in Fig. 7 corresponds to direct electrical modulation of the channel from the back gate.

An electromechanical transconductance of the IG-FinFET is measured at 35 μS (or 159 μS/ μm) for a transistor gate length of 500 nm and gate dielectric of 15 nm silicon nitride, with a gate voltage of 4 V.

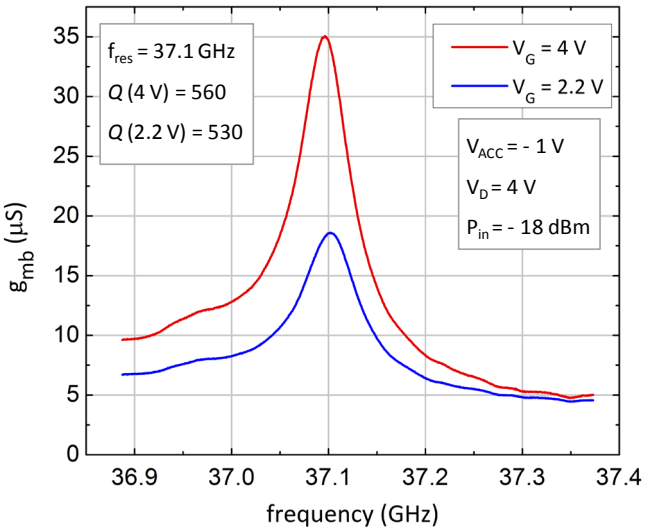

Fig. 7. *Measured frequency response of the IG-FinFET applying gate voltages of 2.2 V and 4 V. The resonance frequency of 37.1 GHz corresponds to the 1st harmonic width-extensional mode of the 114 nm fin. The excitation on the back gate of the IG-FinFET isolates the electrical input and output signals.*

The IG-FinFET exhibits a resonance at 37.1 GHz with a quality factor of $Q = 560$ at a gate voltage of 4 V and $Q = 530$ at a gate voltage of 2.2 V. The resulting $f.Q$ product of 2.1 x 10^{13} is on par with the high $f.Q$ products seen in all internal dielectrically transduced longitudinal-mode bar resonators, in spite of the IG-FinFET's unpatterned gate. The limiting dissipation mechanisms in this device are the acoustic losses due to misalignment of the fin and gate masks as well as the electrical losses through the resistive ungated segment of the fin at the source and drain.

An atomic force microscopy (AFM) scan of the IG-FinFET revealed a fin width of 114 nm, in excellent agreement with 1st harmonic width extensional mode of the fin at 37 GHz.

CONCLUSION

The electromechanical resonance of transistors enables internal amplification of the desired mechanical signal, greatly improving the dynamic range of GHz-frequency MEMS devices above the parasitic capacitance floor. This sensing mechanism allows for detection of acoustic resonance at previously inaccessible frequencies. A freely-suspended IG-FinFET was implemented as a Resonant Body Transistor, demonstrating an acoustic resonance frequency of 37.1 GHz and quality factor of 560. The hybrid NEMS-CMOS RBT will provide a small-footprint, low-power, high sensitivity building block for many RF and mm-wave applications.

ACKNOWLEDGMENTS

This work was funded by Army Research Labs. The authors thank Wentao Wang of MIT for providing COMSOL simulations of the device. Devices were fabricated at the Cornell Nanoscale Science and Technology Facility (CNF), a member of the NNIN.

REFERENCES

[1] H.C. Nathanson, W.E. Newell, R.A. Wickstrom, J.R. Davis Jr., "The resonant gate transistor," *IEEE Transactions on Electron Devices* **1967,** *14* (3)*,* 117-133.

[2] C. Durand, F. Casset, P. Renaux, N. Abele, B. Legrand, D. Renaud, E. Ollier, P. Ancey, A.M. Ionescu, L. Buchaillot, "In-plane silicon-on-nothing nanometer-scale resonant suspended gate MOSFET for in-IC integration perspectives," *Electron Device Letters* **2008**, *29* (5), 494-496.

[3] E. Colinet, C. Durand, L. Duraffourg, P. Audebert, G. Dumas, F. Casset, E. Ollier, P. Ancey, J.-F. Carpentier, L. Buchaillot, A.M. Ionescu, "Ultra-sensitive capacitive detection based on SGMOSFET compatible with front-end CMOS process," *Journal of Solid-State Circuits* **2009**, *44* (1), 247-257.

[4] D. Grogg, M. Mazza, D. Tsamados, A.M. Ionescu, "Multi-gate vibrating-body field-effect transistors (VB-FETs)," *IEEE IEDM* **2008**, 1-4.

[5] Kim, H.S.; Qin, H.; Blick, R.H., "Direct mechanical mixing in a nanoelectromechanical diode," *Applied Physics Letters* **2007**, *91*, 143101.

[6] M. Faucher, B. Grimbert, Y. Cordier, N. Baron, A. Wilk, H. Lahreche, P. Bove, M. François, P. Tilmant, T. Gehin, C. Legrand, M. Werquin, L. Buchaillot, C. Gaquière, D. Théron, "Amplified piezoelectric transduction of nanoscale motion in gallium nitride electromechanical resonators," *Applied Physics Letters* **2009**, *94*, 233506.

[7] D. Weinstein, S.A. Bhave, "Internal dielectric transduction: optimal position and frequency scaling," *IEEE TUFFC* **2007**, 54(12), pp. 2696-98.

[8] D. Weinstein, S.A. Bhave, S. Morita, S. Mitarai, K. Ikeda, "Frequency scaling and transducer efficiency in internal dielectrically transduced silicon bar resonators," *Transducers* **2009**, pp. 708-711.

[9] D. Weinstein, S.A. Bhave, "Internal dielectric transduction of a 4.5 GHz silicon bar resonator," *IEEE IEDM* **2007**, pp.415-418.

[10] D. Weinstein, S.A. Bhave, "The resonant body transistor" *Nano Letters ASAP* **2010**. DOI: 10.1021/nl9037517

[11] D.M. Fried, J.S. Duster, K.T. Kornegay, "High-performance p-type independent-gate FinFETs," *IEEE Electron Device Letters* **2004**, 25(4), pp. 199-201.

CONTACT

*D. Weinstein, tel: +1-617-253-8930; dana@mtl.mit.edu